

## Hole concentration in the three-CuO<sub>2</sub>-plane copper-oxide superconductor Cu-1223

M. Karppinen,<sup>a,\*</sup> H. Yamauchi,<sup>a</sup> Y. Morita,<sup>a</sup> M. Kitabatake,<sup>a</sup> T. Motohashi,<sup>a</sup> R.S. Liu,<sup>b</sup> J.M. Lee,<sup>c</sup> and J.M. Chen<sup>c</sup>

<sup>a</sup> *Materials and Structures Laboratory, Tokyo Institute of Technology, 4259 Nagatsuta, Midori-ku, Yokohama 226-8503, Japan*

<sup>b</sup> *Department of Chemistry, National Taiwan University, Taipei, Taiwan, ROC*

<sup>c</sup> *National Synchrotron Radiation Research Center, Hsinchu, Taiwan, ROC*

Received 29 July 2003; accepted 13 October 2003

### Abstract

Strongly overdoped samples of the three-CuO<sub>2</sub>-plane copper-oxide superconductor, CuBa<sub>2</sub>Ca<sub>2</sub>Cu<sub>3</sub>O<sub>8+z</sub> or Cu-1223, were obtained through high-pressure synthesis and post-annealed to various hole-doping levels so as to have the value of  $T_c$  range from 65 to 118 K. A concomitant decrease in the average valence of copper from  $\sim 2.20$  to  $\sim 2.05$  was evidenced by means of wet-chemical and thermogravimetric analyses and Cu  $L$ -edge X-ray absorption near-edge structure (XANES) spectroscopy. The valence value as low as  $\sim 2.05$  that corresponds to the highest  $T_c$  ( $= 118$  K) may be understood by taking into account multiple ways for holes to be distributed among the different Cu–O layers. In terms of actual chemical composition of the Cu-1223 phase, both Cu  $L$ -edge and O  $K$ -edge XANES results suggest that some portion of charge-reservoir copper atoms may have been replaced by CO, i.e., (Cu<sub>1-x</sub>C<sub>x</sub>)Ba<sub>2</sub>Ca<sub>2</sub>Cu<sub>3</sub>O<sub>8+x+z</sub>. The variation range of excess oxygen was estimated at  $\Delta z \approx 0.3$ .

© 2003 Elsevier Inc. All rights reserved.

**Keywords:** Cu-1223 high- $T_c$  superconductor; Oxygen content; Hole concentration; Wet-chemical analysis; Thermogravimetry; XANES spectroscopy

### 1. Introduction

The indispensable role of CuO<sub>2</sub> plane(s) in the occurrence of high- $T_c$  superconductivity has been well established. Moreover, the concentration of holes in these plane(s) sensitively controls the superconductivity characteristics, e.g., the superconductivity transition temperature ( $T_c$ ) and the irreversibility field of magnetization ( $H_{irr}$ ), of high- $T_c$  superconductive copper-oxide compounds as expressed by  $M_m A_2 Q_{n-1} Cu_n O_{m+2+2n\pm\delta}$  or  $M-m2(n-1)n$  [1]. Here  $M$  (= e.g., Cu, Bi, Pb, Tl, Hg, C) refers to the cation in the oxygen-nonstoichiometric  $M_m O_{m\pm\delta}$  “charge-reservoir” block,  $A$  (= e.g., Ba, Sr) refers to the cation in the oxygen-stoichiometric  $AO$  layer located between an  $MO_{1\pm\delta/m}$  layer and a CuO<sub>2</sub> plane, and  $Q$  (= e.g., Ca, Y) is the constituent of the oxygen-free cation layer separating each two CuO<sub>2</sub> planes in the superconductive CuO<sub>2</sub>-( $Q$ -CuO<sub>2</sub>) <sub>$n-1$</sub>  block. In the structure of an  $M-m2(n-1)n$  phase,

CuO<sub>2</sub> plane(s) thus alternate with the  $MO_{1\pm\delta/m}$ ,  $AO$  and  $Q$  layers according to a general sequence, CuO<sub>2</sub>-( $Q$ -CuO<sub>2</sub>) <sub>$n-1$</sub> - $AO$ -( $MO_{1\pm\delta/m}$ ) <sub>$m$</sub> - $AO$ .

Among the variety of high- $T_c$  superconductive phases, those that possess a common  $AO$ -( $MO_{1\pm\delta/m}$ ) <sub>$m$</sub> - $AO$  portion, i.e., “blocking block”, form a homologous series, and among the members of each homologous series, the highest  $T_c$  belongs to the  $n = 3$  member [1]. The most thoroughly characterized superconductive compound, i.e., the so-called “Y-123” or YBa<sub>2</sub>Cu<sub>3</sub>O<sub>6+z</sub>, has a multi-layered structure of the layer sequence, CuO<sub>2</sub>-Y-CuO<sub>2</sub>-BaO-CuO <sub>$z$</sub> -BaO, with a single CuO <sub>$z$</sub>  chain functioning as the charge reservoir (henceforth we use “ $z$ ” instead of “ $1\pm\delta$ ” to refer to the amount of oxygen in the charge reservoir); The structure of YBa<sub>2</sub>Cu<sub>3</sub>O<sub>6+z</sub> is thus expressed as Cu-1212 [1]. The initial dream to insert additional CuO<sub>2</sub> planes (and additional  $Q$  layers to fulfill the charge-neutrality condition) into the middle of the Cu-1212 unit cell structure in order to increase  $T_c$  came true when the  $n = 3-6$  phases of the CuBa<sub>2</sub>Ca <sub>$n-1$</sub> Cu <sub>$n$</sub> O<sub>2+2n+z</sub> or Cu-12( $n-1$ ) $n$  system were discovered utilizing high-pressure

\*Corresponding author. Fax: +81-45-924-5365.

E-mail address: [karppinen@msl.titech.ac.jp](mailto:karppinen@msl.titech.ac.jp) (M. Karppinen).

(HP) synthesis techniques [2,3]. Later it was revealed that part/half of the charge-reservoir  $\text{CuO}_z$  units in the  $\text{CuBa}_2\text{Ca}_{n-1}\text{Cu}_n\text{O}_{2+2n+z}$  phases can be replaced by CO units that together with the apical oxygen atoms form carbonate groups,  $[\text{C}^{\text{IV}}\text{O}_3]^{2-}$  [4]. As expected, the highest value of  $T_c$  in the Cu-12(n-1)n series, i.e.,  $\sim 120$  K, was found to belong to the optimized Cu-1223 phase [5]. Samples of the Cu-1223 phase obtained through HP synthesis are strongly overdoped [5,6], in contrast to the fully oxygenated Cu-1212 phase which is rather close to the optimum hole-doping level. This is due to the fact that the  $Q$ -metal site in the superconductive  $\text{CuO}_2-(Q-\text{CuO}_2)_{n-1}$  block is occupied by divalent Ca in Cu-1223 but by trivalent Y in Cu-1212. Here it is useful to recognize that even at  $z=0$ , the average valence of copper in Cu-1223 ( $\text{CuBa}_2\text{Ca}_2\text{Cu}_3\text{O}_{8+z}$ ) is as high as +2.00, while it is +1.67 in Cu-1212 ( $\text{CuBa}_2\text{YCu}_2\text{O}_{6+z}$ ).

Even though the three- $\text{CuO}_2$ -plane copper oxides show the highest  $T_c$  values, these phases are rather poorly understood in terms of the degree of hole doping. Among the three- $\text{CuO}_2$ -plane phases, Cu-1223 shows the largest variation in  $T_c$ : removal of oxygen from the strongly overdoped as-HP-synthesized Cu-1223 samples increases the  $T_c$  value from  $\sim 67$  up to 120 K [5,6]. The Cu-1223 phase is thus an interesting target for a quantitative hole-doping study. Here we utilize wet-chemical and thermogravimetric (TG) analyses as well as Cu  $L$ -edge and O  $K$ -edge X-ray absorption near-edge structure (XANES) spectroscopy to estimate the concentration of holes in a series of Cu-1223 samples post-annealed to various doping levels. Due to the dipole selection rule, the Cu  $L_{2,3}$ -edge absorption spectrum is governed by transitions from the Cu  $2p_{1/2,3/2}$  core levels into the hole states of Cu  $3d$  character. On the other hand, in the O  $K$ -edge spectra, the O  $2p$  hole states are accessible.

## 2. Experimental

Five  $\text{CuBa}_2\text{Ca}_2\text{Cu}_3\text{O}_{8+z}$  samples with different oxygen contents were prepared by means of (i) HP synthesis to obtain the Cu-1223 phase, and (ii) subsequent TCO (temperature-controlled oxygen depletion) annealings to gradually remove excess oxygen. A cation-stoichiometric powder mixture of  $\text{CuO} + 2\text{BaCuO}_{2.15} + \text{Ca}_2\text{CuO}_3$  was used as a precursor for the HP synthesis. Precursors,  $\text{BaCuO}_{2.15}$  [8] and  $\text{Ca}_2\text{CuO}_3$ , were synthesized *prior* to use from  $\text{BaCO}_3$ ,  $\text{CaCO}_3$  and  $\text{CuO}$  by firing at  $850^\circ\text{C}$  and  $950^\circ\text{C}$ , respectively, for 25 h in flowing  $\text{O}_2$  gas. The precursor materials were mixed together with 100 mol%  $\text{Ag}_2\text{O}_2$ , i.e., 1 mol of  $\text{Ag}_2\text{O}_2$  for every mol of Cu-1223, and pressed at 5 GPa in a cubic-anvil-type pressure apparatus at  $1100^\circ\text{C}$  for 30 min. The function of  $\text{Ag}_2\text{O}_2$  was to act as an excess-oxygen source

during synthesis. The four oxygen-deficient samples were prepared from the as-HP-synthesized Cu-1223 material by TCO annealings carried out in a thermobalance (MAC Science: TG/DTA 2000 S) in flowing Ar gas at temperatures of  $300^\circ\text{C}$ ,  $360^\circ\text{C}$ ,  $420^\circ\text{C}$ , and  $500^\circ\text{C}$ . These post-annealed samples are referred to as “Ar-300”, “Ar-360”, “Ar-420” and “Ar-500” samples. Note that for Cu-1223,  $500^\circ\text{C}$  is close to the phase decomposition temperature in Ar.

As the TCO annealings were carried out for small powder samples ( $\sim 50$  mg) using a slow heating rate ( $2^\circ\text{C}/\text{min}$ ) and employing an isothermal heating period of 8 h at the final temperature, the obtained samples were considered to be highly homogeneous in terms of the spatial distribution of oxygen. Moreover, since each TCO annealing was carried out in a thermobalance of high sensitivity with in situ TG detection of the weight change, a good estimation of the amount of depleted oxygen was obtained for the annealed samples. The exact oxygen contents were further established by coulometric  $\text{Cu}^+/\text{Cu}^{2+}$  titrations [1,7] using a special “microtitration” technique [9] that allows relatively accurate determination of the oxygen content in a sample of a mass as small as  $\sim 10$  mg. Powder X-ray diffraction measurements (XRD; MAC Science: MXP18VAHF<sup>22</sup>;  $\text{CuK}\alpha$  radiation) were applied to check phase purity and determine the lattice parameters for all the samples. The  $T_c$  values reported for the samples were taken at the onset temperatures of diamagnetic signal in SQUID measurements (Quantum Design: MPMS-XL) carried out down to 5 K in a field-cooling mode with a magnetic field of 10 Oe.

The Cu  $L$ -edge and O  $K$ -edge XANES measurements were performed for powder samples according to a well-established routine [10,11] in the bulk-sensitive X-ray fluorescence-yield mode on 6-m High-Energy Spherical Grating Monochromator (HSGM) beam-line at National Synchrotron Radiation Research Center (NSRRC) in Hsinchu, Taiwan. The spectra were recorded at room temperature using a micro-channel-plate (MCP) detector system consisting of a dual set of MCPs with an electrically isolated grid mounted in front of them. The grid was set to a voltage of 100 V, the front of the MCPs to  $-2000$  V and the rear to  $-200$  V. The grid bias ensured that positive ions did not enter the detector, while the MCP bias ensured that no electrons were detected. The detector was located parallel to the sample surface at a distance of  $\sim 2$  cm. Photons were incident at an angle of  $45^\circ$  in respect to the sample normal. The incident photon flux was monitored simultaneously by a Ni mesh located after the exit slit of the monochromator. The photon energies were calibrated with an accuracy of 0.1 eV using the Cu  $L_3$  white line at 931.2 eV and the O  $K$ -edge absorption peak at 530.1 eV of a CuO reference. The monochromator resolution was set to  $\sim 0.22$  eV for the O  $K$ -edge energy

region and  $\sim 0.45$  eV for the Cu *L*-edge energy region. The obtained spectra were corrected for the energy-dependent incident photon intensity variation as well as for self-absorption effects [12,13] and normalized to tabulated standard absorption cross sections [14] in the energy range of 600–620 eV for the O *K* edge and 1000–1020 eV for the Cu *L* edge.

### 3. Results and discussion

Judging from the X-ray diffraction data the synthesized  $\text{CuBa}_2\text{Ca}_2\text{Cu}_3\text{O}_{8+z}$  samples were of high-quality but not totally free from secondary phases, see the XRD pattern in Fig. 1 for the as-HP-synthesized sample. Besides those from the Cu-1223 main phase, diffraction peaks originating from small amounts of CuO and an unidentified impurity phase were detected in all the samples with unchanged intensities and  $2\theta$  values. Furthermore, the synthesis product contained a reduction residue of  $\text{Ag}_2\text{O}_2$  used as the oxygen source, presumably in the form of oxygen-deficient high-pressure form of silver oxide [15]. Here note that with preliminary TEM-EDX analysis we had confirmed that under the presently applied synthesis conditions Ag atoms do not enter the Cu-1223 structure. Upon TCOD annealing, the silver oxide residue decomposes to metallic silver below  $300^\circ\text{C}$  [6]. Consequently, peaks due to metal Ag appeared in the XRD patterns for all the TCOD-annealed, oxygen-depleted Cu-1223 samples.

From the TG curves recorded for TCOD annealings oxygen evolution was revealed to start around  $300^\circ\text{C}$ .

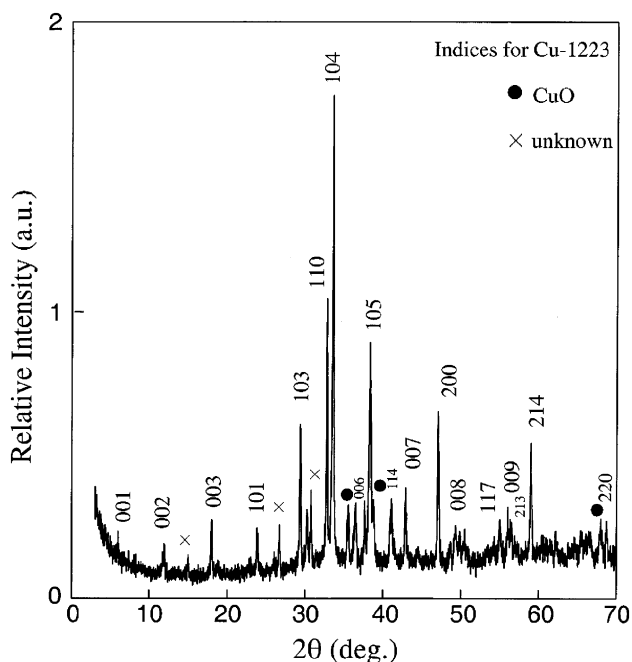


Fig. 1. Powder X-ray diffraction pattern recorded for an as-HP-synthesized  $\text{CuBa}_2\text{Ca}_2\text{Cu}_3\text{O}_{8+z}$  (Cu-1223) sample.

The decomposition of the silver oxide residue to metal Ag and the oxygen evolution from the Cu-1223 phase occur in two distinct steps, i.e., the decomposition reaction of the silver oxide is completed before the oxygen evolution from Cu-1223 starts [6]. This enables us to make relatively accurate estimations for the amount of oxygen depleted from the Cu-1223 phase based on the TG curves. For TCOD annealing carried out at  $500^\circ\text{C}$  the amount of oxygen removed from the HP-synthesized Cu-1223 material was calculated at  $\Delta z \approx 0.3$ . For the other annealings performed at lower temperatures the amount of removed oxygen was accordingly less. Moreover, the absolute amount of excess oxygen,  $z$ , in the  $\text{CuO}_z$  charge reservoir was estimated for the TCOD-annealed Cu-1223 samples from the wet-chemical redox analysis based on coulometric  $\text{Cu}^+/\text{Cu}^{2+}$  titrations.<sup>1</sup> The  $z$  values given in Table 1 are average values from three parallel experiments. Note that for the as-HP-synthesized sample no wet-chemical analysis was performed due to the additional (nonstoichiometric) silver oxide phase contained in the sample, but the value of  $z$  given in Table 1 was indirectly estimated based on (i) the observed amount of oxygen lost upon the TCOD annealing when preparing the Ar-500 sample from the as-HP-synthesized material, and (ii) the oxygen content of the Ar-500 sample as determined from a wet-chemical analysis. Owing to the lack of perfect phase purity, the error bars for  $z$  were estimated at  $\pm 0.05$ . Nonetheless, the results of chemical analyses confirmed the fact that the oxygen content gradually decreased upon increasing TCOD annealing temperature and also that the amount of removable oxygen was approximately at the level of  $\Delta z \approx 0.3$ . An estimation for the average valence of copper,  $V(\text{Cu})_z$ , was calculated as:

$$V(\text{Cu})_z = 2 + 0.5z \quad (1)$$

from the value determined for the excess oxygen,  $z$ , taking a charge-neutrality condition into account and assuming integer valence values for all other elements except for copper. The obtained values are given in Table 1. Upon oxygen depletion,  $V(\text{Cu})_z$  decreases from 2.20(3) to 2.06(3). In Table 1, we also give the value of  $T_c$  and the *c*-axis lattice parameter for all the samples. The decrease in oxygen content is reflected in the gradual increase in the *c*-axis lattice parameter. With decreasing oxygen content,  $T_c$  increases in a continuous manner as anticipated from a previous study [6], manifesting the overdoped state of the samples.

The Cu *L*-edge absorption spectra for the samples are shown in Fig. 2. For all the samples a narrow peak centered about 931.2 eV covers most of the spectral

<sup>1</sup> Metallic Ag contained in the sample does not interfere with the wet-chemical analysis as long as the weighed mass of the analyzed sample is “corrected” for the amount of Ag.

Table 1  
Experimental data for the present  $\text{CuBa}_2\text{Ca}_2\text{Cu}_3\text{O}_{8+z}$  (Cu-1223) samples

Sample	$T_c$ (K)	$c$ (Å)	$z$	$V(\text{Cu})_z$	$V(\text{Cu})_{\text{XAS}}$	$I(\text{holes})_{\text{XAS}}$ (Mb-eV)
HP-syn	65	14.75	0.40(5)	2.20(3)	2.18(3)	0.82(5)
Ar-300	75	14.75	0.27(5)	2.14(3)	2.12(3)	0.77(5)
Ar-360	87	14.76	0.15(5)	2.08(3)	2.13(3)	0.74(5)
Ar-420	100	14.77	0.11(5)	2.06(3)	2.05(3)	0.66(5)
Ar-500	118	14.80	0.13(5)	2.07(3)	2.03(3)	0.58(5)

$T_c$ ,  $c$ -axis parameter, amount of excess oxygen ( $z$ ), average valence of copper as calculated from the analyzed value of  $z$  [ $V(\text{Cu})_z$ ] and from the Cu  $L_3$ -edge XANES data [ $V(\text{Cu})_{\text{XAS}}$ ], and the integrated intensity of the 528.2-eV pre-edge peak in the O  $K$ -edge XANES spectra [ $I(\text{holes})_{\text{XAS}}$ ]. Note that  $I(\text{holes})_{\text{XAS}}$  reflects the overall hole-doping level of the sample.

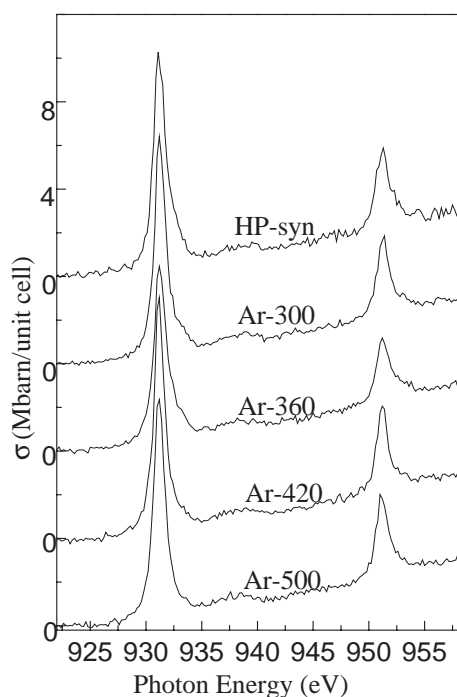


Fig. 2. Cu  $L$ -edge XANES spectra for the Cu-1223 samples.

weight. The same peak has been seen at 931.3 eV in  $\text{CuO}$  [16,17] and at 931.2 eV in  $\text{La}_2\text{CuO}_4$  [18], and it is thus assigned to divalent copper,  $\text{Cu}^{\text{II}}$ , i.e., transitions from the  $\text{Cu}(2p_{3/2})3d^9$  ground state to the  $\text{Cu}(2p_{3/2})^{-1}3d^{10}$  excited state [where  $(2p_{3/2})^{-1}$  denotes a  $2p_{3/2}$  hole]. For the as-HP-synthesized sample, the 931.2 eV peak is clearly asymmetric having a shoulder at a high-energy side, i.e., at  $\sim 932.4$  eV. Such a shoulder has already been observed for a number of  $p$ -type doped superconductive copper-oxide phases, e.g.,  $\text{Cu-1212}$  [11, 19–21], 0201 [22],  $\text{Bi-22}(n-1)n$  [23–26],  $\text{Tl-22}(n-1)n$  [27,28],  $\text{Hg-12}(n-1)n$  [29–31],  $(\text{Tl}_{1/2}\text{Pb}_{1/2})\text{-1212}$  [10] and  $(\text{Pb}_{2/3}\text{Cu}_{1/3})\text{-3212}$  [32]. It has been assigned to trivalent copper,  $\text{Cu}^{\text{III}}$ , and interpreted as transitions from the  $\text{Cu}(2p_{3/2})3d^9\bar{L}$  ground state into the  $\text{Cu}(2p_{3/2})^{-1}3d^{10}\bar{L}$  excited state (where  $\bar{L}$  denotes a ligand hole in the O  $2p$  orbital). In the “ $\text{Cu}^{\text{III}}$  compound”,  $\text{La}_2\text{Li}_{0.5}\text{Cu}_{0.5}\text{O}_{3.96}$ , instead of such a shoulder, a distinct peak due to

trivalent copper is seen at 933.45 eV [18]. For the Cu-1223 phase the relative intensity of the shoulder is supposed to reflect the total concentration of holes, i.e., holes in the three  $\text{CuO}_2$  planes and/or the  $\text{CuO}_z$  charge reservoir. For the TCOD-annealed samples, the shoulder becomes less prominent as the oxygen depletion proceeds. Nevertheless, with decreasing  $z$ , no distinguishable spectral features appear around 934 eV (Fig. 2), that are expected for two-fold-coordinated monovalent Cu species. Such a feature is clearly seen not only for oxygen-deficient samples of Cu-1212 [11,20,21] and  $(\text{Pb}_{2/3}\text{Cu}_{1/3})\text{-3212}$  [32] superconductors but also for  $\text{Cu}_2\text{O}$  [16,17] containing  $\text{Cu}^{\text{I}}$  in a linear coordination. On the other hand, for the  $(R_{1-x}\text{Ce}_x)_2\text{CuO}_4$  system ( $R=\text{Nd, Sm}$ ) with the copper atom in four-fold coordination no peak is seen around 934 eV even though the  $\text{Ce}^{\text{IV}}$ -for- $R^{\text{III}}$  substitution decreases the valence of Cu below II [33]. In the case of the present Cu-1223 samples, a plausible explanation for the absence of the “934-eV” peak is that some portion of the charge-reservoir  $\text{Cu}^{\text{I}}$  species have been replaced by CO units, i.e.,  $(\text{Cu}_{1-x}\text{C}_x)\text{Ba}_2\text{Ca}_2\text{Cu}_3\text{O}_{8+x+z}$ .<sup>2</sup> Such a substitution of monovalent Cu with tetravalent C would bring the oxygen atoms of the CO units close enough to the remaining Cu atoms to break down their linear coordination. The fact that CuO was detected as an impurity in all the HP synthesis products even though a stoichiometric cation composition was used for the synthesis supports this explanation. Unfortunately, neither the presence nor the absence of carbon in the Cu-1223 phase could be clearly confirmed since possibilities for nanoscale detection of carbon are rather limited, a reason why results of such analyses have not been reported so far.

Quantitative analysis of the spectral features in the  $L_3$  area of the Cu  $L$ -edge spectra was carried out to get an estimation independent of that of  $V(\text{Cu})_z$  for the average valence of Cu in the samples. First the background, fitted with an arctangent curve, was subtracted from the spectra. Fitting of the white line at  $\sim 931.2$  eV

<sup>2</sup>From the wet-chemical analysis the magnitude of  $z$ , not  $x+z$ , is obtained.

(Cu<sup>II</sup>) was done using a combination of Lorentzian and Gaussian functions to account for the intrinsic and experimental broadenings, respectively. For the peak at  $\sim 932.4$  (Cu<sup>III</sup>) Gaussian function was applied. The average valence of Cu [ $V(\text{Cu})_{\text{XAS}}$ ] was calculated as:

$$V(\text{Cu})_{\text{XAS}} = 2 + I(\text{Cu}^{\text{III}})/[I(\text{Cu}^{\text{II}}) + I(\text{Cu}^{\text{III}})] \quad (2)$$

from the thus obtained integrated intensities of the “931.2-eV” peak and its shoulder, i.e.,  $I(\text{Cu}^{\text{II}})$  and  $I(\text{Cu}^{\text{III}})$ , respectively. The results are given in Table 1. A good agreement is seen among the values of  $V(\text{Cu})_{\text{XAS}}$  and  $V(\text{Cu})_z$ .

The O *K*-edge absorption spectra of the samples are shown in Fig. 3. The lower-energy pre-edge peak at  $\sim 528.2$  eV is attributed to the excitation of O 1s electrons to O 2p holes in the CuO<sub>2</sub> planes in an analogy to previous studies on various high- $T_c$  superconductive copper oxides [10–12,20–22,25–27,29,31]. The O 2p hole states hybridized with the upper Hubbard band (UHB) are seen about 530 eV. The possible hole states at the oxygen atom in the CuO<sub>z</sub> charge reservoir should coincide with the  $\sim 528.2$ -eV peak if an analogy to the Cu-1212 phase [11,20,21] (with perovskite-type charge reservoir) is expected. However, since the precise charge-reservoir structure of the Cu-1223 phase is not known, the CuO<sub>z</sub> charge-reservoir hole states might also coincide with the UHB peak in an analogy to the three-CuO<sub>2</sub>-plane superconductor, Hg-1223 [29,31] (with rock-salt-type charge reservoir). Here we fitted the total spectral weight in the 527–529 eV energy range to a Gaussian function. The background within 527–529 eV was fitted with a straight line and subtracted from the

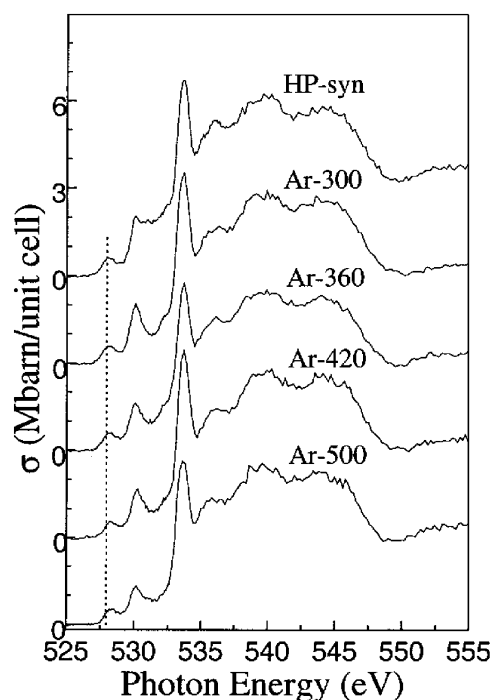


Fig. 3. O *K*-edge XANES spectra for the Cu-1223 samples.

spectra. The integrated intensity,  $I(\text{holes})_{\text{XAS}}$ , that is obtained from the fitting is supposed to reflect the overall hole-doping level in the sample. The results are given in Table 1. As expected, with decreasing oxygen content,  $I(\text{holes})_{\text{XAS}}$  gradually decreases. Another indicator of the decrease in the hole concentration is the fact that the position of the “528.2-eV” peak was found to slightly shift towards the higher energy (see Fig. 3). An additional prominent feature in the O *K*-edge spectra, seen for all the present Cu-1223 samples with an unchanged intensity, is the narrow peak centered at  $\sim 533.8$  eV. One might argue that this peak has its origin in oxygen atoms that belong to the charge-reservoir carbonate groups, though it should be noted that quite a similar peak located about 533.8 eV and assumed to originate from Sr–O hybrids has been observed for some non-CuO<sub>2</sub>-plane copper oxides, e.g., the so-called “one-leg” and “two-leg” ladder compounds, SrCuO<sub>2</sub> and Sr<sub>14</sub>Cu<sub>24</sub>O<sub>41</sub>, that are not expected to contain carbon [34,35].

The  $V(\text{Cu})_z$  and  $V(\text{Cu})_{\text{XAS}}$  values as given in Table 1 were calculated (i) on the basis of 100% phase purity (except for the presence of the reduction residue of Ag<sub>2</sub>O<sub>2</sub>), (ii) ignoring the possible carbon contamination, and (iii) assuming the same valence value for each crystallographically different copper atom. The thus obtained results suggest a rather low  $V(\text{Cu})$  value of approximately 2.05 for the sample with the highest  $T_c$  (= 118 K). To rationalize this, we first confirmed that the values obtained for  $V(\text{Cu})_z$  and  $V(\text{Cu})_{\text{XAS}}$  are not sensitively affected by our choice of cation composition, CuBa<sub>2</sub>Ca<sub>2</sub>Cu<sub>3</sub>O<sub>8+z</sub> or (Cu<sub>1-x</sub>Cu<sub>x</sub><sup>IV</sup>)Ba<sub>2</sub>Ca<sub>2</sub>Cu<sub>3</sub>O<sub>8+x+z</sub> + xCu<sup>II</sup>O [see footnote 2], for the basis of calculation: essentially equal numbers in terms of the average copper valence in the Cu-1223 phase were obtained for  $x = 0$  and 0.5. In other words, the interpretation of our experimental results does not depend on whether or not some carbonate exists in the Cu-1223 structure. Next we considered the possible inhomogeneity in distribution of holes among the different Cu–O layers. In the oxygen-depleted Cu-1223 samples the charge-reservoir copper atoms are likely to possess a valence value not higher than II (in an analogy to the oxygen-depleted Cu-1212 phase). Another fact is that holes may be inhomogeneously distributed among the two types of CuO<sub>2</sub> planes, i.e., inner and outer planes, within the superconductive CuO<sub>2</sub>(outer)–Ca–CuO<sub>2</sub>(inner)–Ca–CuO<sub>2</sub>(outer) block [1]. By attributing all the trivalent copper states to the inner CuO<sub>2</sub> plane (with Cu in square-planar coordination), we end up to a “plane-specific”  $V(\text{Cu})_{\text{effective}}$  value of 2.20. Alternatively, assuming that not the inner but the outer CuO<sub>2</sub> planes (with Cu in pyramidal coordination) are predominantly oxidized gives us a value of 2.10 for  $V(\text{Cu})_{\text{effective}}$ . Unfortunately, by means of the experimental techniques employed it is impossible to gain direct information on how the extra positive

charge/holes are in reality distributed among the different Cu–O layers. Thus, based on the present data we only argue that it is likely that the holes are more or less inhomogeneously distributed between the outer and inner CuO<sub>2</sub> planes of the superconductive block at least in our most deoxygenated Ar-500 Cu-1223 sample.

#### 4. Conclusions

For superconductive multi-layered copper oxides,  $M\text{-}m2(n-1)n$ , concentration of holes in a CuO<sub>2</sub> plane(s) is an important parameter since it controls the superconductivity characteristics. Among the  $M\text{-}m2(n-1)n$  phases, those with a three-CuO<sub>2</sub>-plane structure show the highest  $T_c$  values. However, these phases have been rather poorly characterized in terms of the degree of hole doping. In the present work, we were able to probe the changes in the average valence of copper/CuO<sub>2</sub>-plane hole concentration for a series of Cu-1223 (CuBa<sub>2</sub>Ca<sub>2</sub>Cu<sub>3</sub>O<sub>8+z</sub>) samples post-annealed to various widely ranging doping levels ( $\Delta z \approx 0.3$ ). The studied three-CuO<sub>2</sub>-plane phase is the next-higher homologue to the prototype superconductor, YBa<sub>2</sub>Cu<sub>3</sub>O<sub>6+z</sub> of the Cu-1212 phase. The two independent experimental tools employed, i.e., wet-chemical redox analysis and XANES spectroscopy, gave highly agreeable results. As a manifestation of the increase in the value of  $T_c$  from 65 to 118 K the average valence of copper was found to decrease from  $\sim 2.20$  to  $\sim 2.05$  upon depleting the excess oxygen gradually out from the Cu-1223 phase. The trend of decreasing copper valence with increasing  $T_c$  was what had been expected for a series of overdoped samples, but the value as low as  $\sim 2.05$  revealed for the sample with the highest  $T_c$  (118 K) was considered unexpectedly small. Such a low value of average copper valence is, however, well understood by taking into account that the holes are likely to be inhomogeneously distributed among the inequivalent CuO<sub>2</sub> planes in the superconductive block. Finally, both the Cu  $L$ -edge and the O  $K$ -edge XANES results together with the fact that an excess of CuO was always seen as an impurity in stoichiometric samples gave a positive indication that in our Cu-1223 samples part/half of the charge-reservoir copper atoms might have been replaced by carbon/carbonate, i.e.,  $x > 0$  in (Cu<sub>1-x</sub>C<sub>x</sub>)Ba<sub>2</sub>Ca<sub>2</sub>Cu<sub>3</sub>O<sub>8+x+z</sub>.

#### Acknowledgments

This work was supported by Grant-in-Aid for Scientific Research (contract No. 11305002) from the Ministry of Education, Science and Culture of Japan. Y. Yasukawa is thanked for her help in microtitration analysis.

#### References

- [1] M. Karppinen, H. Yamauchi, Mater. Sci. Eng. R 26 (1999) 51.
- [2] M.A. Alario-Franco, C. Chaillout, J.J. Capponi, J.L. Tholence, B. Souleite, Physica C 222 (1994) 243.
- [3] C.-Q. Jin, S. Adachi, X.-J. Wu, H. Yamauchi, S. Tanaka, Physica C 223 (1994) 238.
- [4] T. Kawashima, Y. Matsui, E. Takayama-Muromachi, Physica C 224 (1994) 69.
- [5] C. Chaillout, S. Le Floch, E. Gautier, P. Bordet, C. Acha, Y. Feng, A. Sulpice, J.L. Tholence, M. Marezio, Physica C 266 (1996) 215.
- [6] T. Ito, H. Suematsu, K. Isawa, M. Karppinen, H. Yamauchi, Physica C 308 (1998) 9.
- [7] M. Karppinen, H. Yamauchi, Oxygen engineering for functional oxide materials, in: A.V. Narlikar (Ed.), International Book Series: Studies of High Temperature Superconductors, Vol. 37, Nova Science Publishers, New York, 2001, pp. 109–143.
- [8] K. Peitola, K. Fujinami, M. Karppinen, H. Yamauchi, L. Niinistö, J. Mater. Chem. 9 (1999) 465; K. Peitola, M. Karppinen, H. Rundlöf, R. Tellgren, H. Yamauchi, L. Niinistö, J. Mater. Chem. 9 (1999) 2599.
- [9] Y. Yasukawa, H. Yamauchi, M. Karppinen, Appl. Phys. Lett. 81 (2002) 502.
- [10] J.M. Chen, R.S. Liu, W.Y. Liang, Phys. Rev. B 54 (1996) 12587.
- [11] M. Karppinen, H. Yamauchi, T. Nakane, K. Fujinami, K. Lehmus, P. Nachimuthu, R.S. Liu, J.M. Chen, J. Solid State Chem. 166 (2002) 229.
- [12] E. Pellegrin, N. Nücker, J. Fink, S.L. Molodtsov, A. Gutiérrez, E. Navas, O. Strebel, Z. Hu, M. Domke, G. Kaindl, S. Uchida, Y. Nakamura, J. Markl, M. Klauda, G. Saemann-Ischenko, A. Krol, Phys. Rev. B 47 (1993) 3354.
- [13] L. Tröger, D. Arvanitis, K. Baberschke, H. Michaelis, U. Grimm, E. Zschech, Phys. Rev. B 46 (1992) 3283.
- [14] J.J. Yeh, I. Lindau, At. Data Nucl. Data Tables 32 (1985) 1.
- [15] S.S. Kabalkina, S.V. Popova, N.R. Serebryanaya, Sov. Phys. 8 (1964) 972; W. Beesk, P.G. Jones, H. Rumpel, E. Schwarzmann, G.M. Sheldrick, JCS Chem. Commun. 664 (1981); N. Serebryanaya, Sov. Phys. Crystallogr. 32 (1987) 608.
- [16] M. Grioni, J.B. Goedkoop, R. Schoorl, F.M.F. de Groot, J.C. Fuggle, F. Schäfers, E.E. Koch, G. Rossi, J.-M. Esteve, R.C. Karnatak, Phys. Rev. B 39 (1989) 1541.
- [17] M. Grioni, J.F. van Acker, M.T. Czyżyk, J.C. Fuggle, Phys. Rev. B 45 (1992) 3309.
- [18] N. Merrien, L. Coudrier, C. Martin, A. Maignan, F. Studer, A.M. Flank, Phys. Rev. B 49 (1994) 9906.
- [19] A. Bianconi, M. DeSantis, A. Di Ciccio, A.M. Flank, A. Fronk, A. Fontaine, P. Legarde, H.K. Yoshida, A. Kotani, A. Marcelli, Phys. Rev. B 38 (1988) 7196.
- [20] N. Nücker, E. Pellegrin, P. Schweiss, J. Fink, S.L. Molodtsov, C.T. Simmons, G. Kaindl, W. Frentrup, A. Erb, G. Müller-Vogt, Phys. Rev. B 51 (1995) 8529.
- [21] M. Merz, N. Nücker, P. Schweiss, S. Schuppler, C.T. Chen, V. Chakarjan, J. Freeland, Y.U. Idzerda, M. Kläser, G. Müller-Vogt, Th. Wolf, Phys. Rev. Lett. 80 (1998) 5192.
- [22] C.T. Chen, L.H. Tjeng, J. Kwo, H.L. Kao, P. Rudolf, F. Sette, R.M. Fleming, Phys. Rev. Lett. 68 (1992) 2543.
- [23] A.Q. Pham, F. Studer, N. Merrien, A. Maignan, C. Michel, B. Raveau, Phys. Rev. B 48 (1993) 1249.
- [24] N.L. Saini, D.S.-L. Law, P. Pudney, K.B. Garg, A.A. Menovsky, J.J.M. Franse, Phys. Rev. B 52 (1995) 6219.
- [25] M. Karppinen, K. Kotiranta, T. Nakane, S.C. Chang, J.M. Chen, R.S. Liu, H. Yamauchi, Phys. Rev. B 67 (2003) 134522.
- [26] M. Karppinen, S. Lee, J.M. Lee, J. Poulsen, T. Nomura, S. Tajima, J.M. Chen, R.S. Liu, H. Yamauchi, Phys. Rev. B 68 (2003) 54502.

- [27] A. Krol, C.S. Lin, Y.L. Soo, Z.H. Ming, Y.H. Kao, J.H. Wang, M. Qi, G.C. Smith, *Phys. Rev. B* 45 (1992) 10051.
- [28] P. Srivastava, F. Studer, K.B. Garg, Ch. Gasser, H. Murray, M. Pompa, *Phys. Rev. B* 54 (1996) 693.
- [29] E. Pellegrin, J. Fink, C.T. Chen, Q. Xiong, Q.M. Lin, C.W. Chu, *Phys. Rev. B* 53 (1996) 2767.
- [30] B.R. Sekhar, F. Studer, K.B. Garg, Y. Moriwaki, C. Gasser, K. Tanabe, *Phys. Rev. B* 56 (1997) 14809.
- [31] T. Watanabe, N. Kiryakov, J. Poulsen, J.M. Lee, J.M. Chen, R.S. Liu, H. Yamauchi, M. Karppinen, *Physica C* 93 (2003) 392.
- [32] M. Karppinen, M. Kotiranta, H. Yamauchi, P. Nachimuthu, R.S. Liu, J.M. Chen, *Phys. Rev. B* 63 (2001) 184507.
- [33] C.F.J. Flipse, G. van der Laan, A.L. Johnson, K. Kadowaki, *Phys. Rev. B* 42 (1990) 1997.
- [34] M. Knupfer, R. Neudert, M. Kielwein, S. Haffner, M.S. Golden, J. Fink, C. Kim, Z.-X. Shen, M. Merz, N. Nücker, S. Schuppler, N. Motoyama, H. Eisaki, S. Uchida, Z. Hu, M. Domke, G. Kaindl, *Phys. Rev. B* 55 (1997) R7291.
- [35] N. Nücker, M. Merz, C.A. Kuntscher, S. Gerhold, S. Schuppler, R. Neudert, M.S. Golden, J. Fink, D. Schild, S. Stadler, V. Chakarian, J. Freeland, Y.U. Idzerda, K. Conder, M. Uehara, T. Nagata, J. Goto, J. Akimitsu, N. Motoyama, H. Eisaki, S. Uchida, U. Ammerahl, A. Revcolevschi, *Phys. Rev. B* 62 (2000) 14384.